Title

Lgr4 Deletion Delays the Hair Cycle and Inhibits the Activation of Hair Follicle Stem Cells

Permalink

https://escholarship.org/uc/item/16q154k3

Journal

Journal of Investigative Dermatology, 140(9)

ISSN

0022-202X

Authors

Ren, Xiaolin
Xia, Weili
Xu, Peng
et al.

Publication Date

2020-09-01

DOI

10.1016/j.jid.2019.12.034

Peer reviewed

Lgr4 Deletion Delays the Hair Cycle and Inhibits the Activation of Hair Follicle Stem Cells

Xiaolin Ren[1,4], **Weili Xia**[1,4], **Peng Xu**[2], **Hongyang Shen**[1], **Xing Dai**[3], **Mingyao Liu**[1], **Yuling Shi**[2], **Xiyun Ye**[1], **Yongyan Dang**[1]

[1]Shanghai Key Laboratory of Regulatory Biology, Institute of Biomedical Sciences and School of Life Sciences, East China Normal University, Shanghai, China

[2]Department of Dermatology, Shanghai Tenth People's Hospital, Tongji University School of Medicine, Shanghai, China

[3]Department of Biological Chemistry, School of Medicine, University of California, Irvine, California, USA

[4]These authors contributed equally to this work.

Abstract

It is known that LGR4 plays an important role in hair follicle (HF) development, but the impact of LGR4 on the hair cycle is still unclear. In this study, we have found that *K14*-Cre–mediated skin epithelia–specific deletion of *Lgr4* results in delayed anagen entry during the physiological hair cycle and compromised HF regeneration upon transplantation. We show that, although *Lgr4* deletion does not appear to affect the number of quiescent HF stem cells, it leads to reduced numbers of LGR5^{+} and actively proliferating stem cells in the HFs. Moreover, *LGR4*-deficient HFs show molecular changes consistent with decreased mTOR and Wnt signaling but upregulated BMP signaling. Importantly, the reactivation of the protein kinase B pathway by injecting the protein kinase B activator SC79 in *Lgr4*$^{-/-}$ mice can effectively reverse the hair cycle delay. Together, these data suggest that LGR4 promotes the normal hair cycle by activating HF stem cells and by influencing the activities of multiple signaling pathways that are known to regulate HF stem cells. Our study also implicates LGR4 as a potential target for treating hair disorder in the future.

INTRODUCTION

The mammalian hair cycle consists of three distinct stages, anagen, catagen, and telogen, which correspond to growing, regressing, and resting phases, respectively (Schneider et al., 2009). Regeneration of a new hair follicle (HF) is fueled by HF stem cells (HFSCs), located at the follicular bulge region, and their immediate progenies in the secondary hair germ (HG). Upon proper stimuli, quiescent HFSCs become activated to drive anagen onset and begin a new hair cycle (Lee et al., 2014).

Several signaling pathways have been shown to regulate the hair cycle through controlling HFSC activities. Wnt signaling is important for the maintenance, activation, and differentiation of HFSCs, and its dysregulation causes the HFSCs to lose their stemness or fail to be properly activated (Lien and Fuchs, 2014; Lim et al., 2016; Lowry et al., 2005). BMP signaling is critical for maintaining the quiescent nature of HFSCs (Zhang et al., 2006). Furthermore, Wnt/β-catenin, TGF-β, and mTOR pathways counterbalance BMP-mediated repression of HFSC activation (Deng et al., 2015; Oshimori and Fuchs, 2012). Additional factors that control the quiescence or activation of HFSCs remain to be elucidated.

Aged HFSCs are eliminated cyclically from the skin through terminal epidermal differentiation, resulting in prominent aging characteristics such as graying, thinning, and loss of the hair (Matsumura et al., 2016). A recent study reported that alkaline ceramidase 1 protects mice from premature hair loss by maintaining HFSC homeostasis (Lin et al., 2017). Therefore, HFSCs play a role not only in maintaining the normal hair growth cycle and hair renewal but also in preventing premature hair aging.

LGR4, a member of the LGR family of proteins, is important for the development of the male reproductive tract, eyelids, kidney, and bone (Kinzel et al., 2014; Lin et al., 2017; Luo et al., 2009; Siwko et al., 2013). It is also involved in tumor formation and metastasis in multiple tissues such as prostate, breast, and lung (Gong et al., 2015; Liang et al., 2015; Yue et al., 2018). Of particular interest, our previous study showed that LGR4 is crucial for skin carcinogenesis by regulating Wnt/β-catenin signaling (Xu et al., 2016). Moreover, *Lgr4*-deficient mice show partial impairment in HF development (Mohri et al., 2008). However, the possible function of LGR4 in the postnatal hair cycle remains to be examined.

In this study, we identify LGR4 as a critical factor that maintains the normal hair cycle and HF regeneration by promoting LGR5^{+} HSFC activation. *Lgr4* deletion delays the hair cycle and impairs folliculoneogenesis upon cellular grafting and hair growth upon transplantation. *Lgr4* deletion also results in abnormalities in protein kinase B (Akt)/mTOR, Wnt/β-catenin, and BMP signaling, which may contribute to the inhibition of HSFC activation and delay of anagen onset. Together, these findings reveal a role for LGR4 in driving early events in adult HF growth and regeneration.

RESULTS

LGR4 is dynamically expressed in postnatal HFs

Because the $Lgr4^{+/-}$ gene trap mouse strain contains a LacZ reporter downstream of the endogenous $Lgr4$ promoter, we used β-galactosidase staining to characterize the dynamics of LGR4 expression during the hair cycle. Skin samples were taken from $Lgr4^{+/-}$ heterozygous mice at various postnatal days (P): P17, P19, P23, P25, P27, P36, P55, and P65. At the end of first telogen and early anagen (P23), LacZ staining was only observed in HF dermal papilla (DP) (Figure 1a), whereas no staining was observed in the interfollicular epidermis and the other epithelial components of the HF. In mid- or even late-stage second anagen HFs (P27), LGR4 expression was found in the DP, bulge, secondary HG, and sebaceous gland (Figure 1a). As anagen progressed (P36), LGR4 expression was detected in the DP, matrix, inner root sheath, and outer root sheath (Figure 1a). Overall, LGR4 is expressed in most of the epithelial cells of the HF as well as in the DP (Figure 1a). Moreover, semiquantitative analysis for LacZ staining showed that LGR4 expression is higher in anagen (P17 and P36) than in telogen (P23 and P55) (Figure 1b). Quantitative real-time PCR analysis revealed a higher level of $Lgr4$ mRNA in catagen and mid- to late-anagen epidermis than in telogen and early anagen epidermis (Figure 1c). Together, these results reveal a broad but dynamic expression of LGR4 in adult HFs, including appreciable expression in HFSC and progenitor cell compartments.

Lgr4 deficiency delays hair cycle

To determine the function of LGR4 in skin epithelial cells, we generated skin epithelium–specific, constitutive $Lgr4$ knockout mice (hereafter referred to as $Lgr4$cKO mice) to delete $Lgr4$ in all cells of the epidermis and HFs. RT-PCR results showed that the level of $Lgr4$ mRNAs was significantly lower in $Lgr4$cKO epidermis than in the control group (Supplementary Figure S1a).

We next examined if $Lgr4$ deficiency in skin epithelium affects the hair cycle. Despite the smaller body size of $Lgr4$cKO mice, their HFs were able to reach full anagen at P14 just like the control littermates (Figure 2a). However, histological analysis and monitoring skin color change after shaving revealed a significant delay in the transition from first telogen to the subsequent anagen in both male and female mutants (Figure 2a and b; Supplementary Figure S1b).

We also examined the effect of $Lgr4$ deletion on depilation-induced hair regeneration. Hairs on the right dorsal skin of 18-month-old mice were plucked by using waxing, whereas those on the left dorsal skin were shaved as the control. Hair regrowth on the right side was considerably slower in $Lgr4$cKO mice than the same site in the wild-type (WT) mice (Figure 2c). H&E staining also showed a marked delay of anagen entry in the $Lgr4$cKO mice after depilation (Figure 2d). Thus, a functional $Lgr4$ gene is required in skin epithelium for anagen entry during the normal hair cycle and for depilation-induced hair regrowth.

Lgr4 deficiency inhibits HSFC activation

We next examined whether *Lgr4* deletion impacts HFSCs. Flow analysis revealed a similar number of CD34$^+$α6-integrin$^+$ HFSCs in *Lgr4*cKO mice and controls at P25 (Supplementary Figure S1d and e). In contrast, immunofluorescent staining with an antibody against LGR5, a marker for adult HFSCs that are the first to be activated during telogen–anagen transition (Wang et al., 2017), showed that LGR5$^+$ cell number was decreased in the bulge of *Lgr4*cKO mice when compared with littermate controls (Supplementary Figure S1c and f). To further examine changes in LGR5$^+$ cells, we crossed *Lgr4*$^{+/−}$ mice with *Lgr5*-GFP reporter mice to produce *Lgr4* knockout mice with *Lgr5*-GFP reporter (KO-GFP) and WT mice (WT-GFP). Flow cytometry analysis revealed a significant reduction in the number of GFP$^+$ (hence LGR5$^+$) cells in P25 skin of LGR4 mutant mice compared with WT controls (Figure 3a). Indirect immunofluorescence using an anti-GFP antibody confirmed the presence of fewer GFP$^+$ cells in the lower bulge/HG of *Lgr4*cKO HFs (Figure 3b). Additionally, immunofluorescent staining using HG marker P-cadherin detected reduced staining intensity at both P23 and P25 in *Lgr4*cKO mice compared with the WT mice (Figure 3c). In contrast, no marked difference was seen for the expression of DP marker alkaline phosphatase between the *Lgr4*cKO and WT mice (Supplementary Figure S1g). Collectively, these results suggest that the absence of LGR4 specifically affects the proliferating subset of HFSCs, a notion further confirmed by the scarcity of Ki67-positive cells in the lower bulge/HG at a time when such cells were abundant in control counterparts (Figure 3d).

Lgr4 deletion inhibits hair and HF regeneration upon transplantation

Next, we examined the function of LGR4 in hair and HF regeneration using two different transplantation assays (Bartholomew et al., 2002; Ehama et al., 2007). First, we intracutaneously injected dissociated epidermal cells from *Lgr4*$^{−/−}$ or *Lgr4*$^{+/+}$ mice at the age of two months together with fetal dermal cells of WT mice into immunodeficient nude mice (Figure 4a). Compared with *Lgr4*$^{+/+}$ counterparts, epidermal cells from *Lgr4*$^{−/−}$ mice produced significantly reduced numbers of hairs and HFs (Figure 4b and c).

We then grafted skin from control and *Lgr4*cKO mice onto nude mice. There were significantly fewer hairs produced by the *Lgr4*cKO skin compared with the control skin at 3 weeks after transplantation (Figure 4d and e). It is worth noting that no difference in hair length was observed between the *Lgr4*cKO and WT skin transplants (Figure 4f). Together with the data previously described, our findings show that LGR4 is required for optimal regeneration of hairs and HFs under both physiological and transplantation conditions.

Altered activities of multiple signaling pathways (Akt/mTOR, Wnt, and BMP) in *Lgr4*-deficient HFs

Given that mTOR and Wnt signaling pathways facilitate HFSC activation and anagen initiation via counteracting BMP-mediated repression during hair cycle, we next investigated the effect of *Lgr4* deletion on these three signaling pathways. First, the expression of phospho-S6 (p-S6), a marker for the activity of mTOR, was examined by immunostaining. As shown in Figure 5, in the HFs of WT mice, p-S6 showed weak activity at early anagen (P23) and elevated levels at anagen (P25) but was then diminished at a later stage of anagen

(P27). However, p-S6 level was consistently low in the HFs of *Lgr4*cKO mice at P23, P25, and P27 (Figure 5a; Supplementary Figure S2a). Western blot analysis confirmed a marked reduction of p-S6 levels in the epidermis of *Lgr4*cKO mice at P25 compared with the controls (Figure 5b). Even when HFs of the LGR4 mutant mice eventually entered early anagen (P30), they still showed a lower level of p-S6 (Supplemental Figure 2b). Considering that there is no marked structural difference between *Lgr4* WT and cKO mice at P23 (Figure 2a), we sorted CD34$^+$α6-intergrin$^+$ HFSCs at P23 by FACS and examined the expression of downstream genes of the Akt/mTOR signaling pathway in sorted cells. Significant downregulation of *4E-BP1* and *eIF-4E* in *Lgr4*cKO mice was observed (Figure 5c). When we injected Akt activator SC79 into the epidermal-dermal junction of back skin in *Lgr4*cKO mice at telogen (P21), the delayed hair cycle phenotype in these *Lgr4*cKO mice was fully rescued (Figure 5d). Collectively, these results show that *Lgr4* regulates hair cycle progression in part through promoting the activity of Akt/mTOR signaling pathway in the HF.

Next, potential changes in Wnt signaling components in the HFs of *Lgr4*cKO mice was examined. The level of β-catenin was elevated from P23 to P25–P27 in WT HFs (Figure 5e), but stayed low in *Lgr4*cKO HFs at P25, P27, and P30 (Figure 5e; Supplementary Figure S2c and d). Western blot confirmed a reduced level of β-catenin in the epidermis of *Lgr4*cKO mice (Figure 5b). Moreover, the expression of LEF1 was lower in *Lgr4*cKO mice than WT mice at P23, P25, and P27 (Supplementary Figure S2e and f). Even when HFs in *Lgr4*cKO mice reached early anagen (P30), LEF1-positive staining was still weaker than WT mice (Figure 5f). Two well-known downstream target genes of Wnt signaling, *c-Myc* and *Axin2*, were also greatly downregulated in HFSCs of *Lgr4*cKO mice at P23 (Figure 5g). Thus, *Lgr4* deletion also inhibited the activation of Wnt signaling in HFs.

Finally, we examined the effect of *Lgr4* deletion on BMP signaling. Western blot analysis showed that p-SMAD1/5/9 level was higher in *Lgr4*cKO mice than WT mice (Figure 5b). Immunofluorescence results revealed a similar pattern of p-SMAD1/5/9 expression in both *Lgr4*cKO and control HFs, but the signal intensities in the bulge were higher in the former at both telogen and anagen stages (Supplementary Figure S3a and b). Furthermore, PCR analysis revealed reduced expression of downstream target genes of BMP signaling including *Id1*, *Id2*, and *Id3* in HFSCs from *Lgr4*cKO mice (Supplementary Figure S3c). These results suggest that BMP signaling activity is activated in the HF when *Lgr4* is deleted.

DISCUSSION

Germline loss of LGR4 results in reduced viability with developmental defects in many organs including HFs (Mohri et al., 2008; Siwko et al., 2013). In this study, we found that deletion of *Lgr4* in skin epithelial cells delays the physiological hair cycle and compromises hair regeneration upon transplantation. Our findings provide evidence for an important involvement of LGR4 in HFSC activation, which is likely mediated through its impact on known HFSC-regulating signaling pathways including mTOR, Wnt, and BMP. Thus, our work identifies LGR4 as a key regulator of postnatal HF cyclic bouts of growth and regression and HFSC activity.

Surprisingly, *Lgr4* epidermal cKO mice display a dramatic decrease in body size. Although we cannot fully exclude the possibility that hair cycle delay in *Lgr4*cKO mice is an indirect consequence of other causes such as nutrient stress and developmental defect, the results of our grafting and transplantation assays argue strongly for a more direct and skin epithelial cell–intrinsic role of LGR4 in hair and HF growth and regeneration.

It is reported that CD34$^+$ HFSCs have the attributes of quiescence and multipotency, whereas LGR5 marks an actively cycling stem cell population in the HF (Fuchs, 2009; Lin and Yang, 2013; Trempus et al., 2007). HF regeneration is highly dependent on the activation of LGR5$^+$ HFSCs. We found that *Lgr4* deletion decreases the number of LGR5$^+$ HFSCs but not CD34$^+$ HFSCs, and it inhibits HFSC proliferation in the lower bulge and HG. HG cells are derived from bulge stem cells and respond more quickly to hair cycle–promoting signals from the DP (Greco et al., 2009). Thus, our data suggest that LGR4 functions in HF growth and regeneration through activating HFSCs.

R-spondins are endogenous ligands for LGR4 (Carmon et al., 2011). Expression of RSPO1 in the DP is specifically and prominently upregulated before anagen entry, and injection of recombinant R-spondin 1 protein at mid-telogen leads to precocious anagen entry (Li et al., 2016). RSPO2 has also been shown to stimulate hair growth (Smith et al., 2016). LGR4 has been shown to augment Wnt/β-catenin signaling via binding to Wnt agonists R-spondins (Xu et al., 2016). It is also reported that Wnt signal becomes elevated when bulge cells are activated to undergo the transition from telogen to anagen (Lim et al., 2016). Our findings that LGR4 is required for timely HFSC activation and maximal Wnt signaling output and that LGR4 expression is greatly upregulated during telogen-to-anagen transition are consistent with these previous studies. Together they suggest a model in which an R-spondin–LGR4–Wnt signaling pathway operates in the HFSC niche to trigger HFSC activation and anagen entry.

Hair regeneration is also governed by Akt signaling that acts upon HFSCs located in the follicle bulge (Qiu et al., 2017). A recent study shows that macrophages induce Akt/β-catenin–dependent LGR5$^+$ stem cell activation and HF regeneration in skin wounds (Wang et al., 2017). Here, we showed that *Lgr4* deletion also inhibits the activation of Akt/mTOR signaling pathway in the HFs. Reactivation of Akt pathway in *Lgr4* mutant mice reversed their delayed hair cycle, indicating that Akt signaling pathway is critical in LGR4-regulated HF homeostasis and HFSC activation.

BMP signaling has been shown to inhibit HFSC activation, which could be counterbalanced by mTOR signaling during hair follicle regeneration (Deng et al., 2015). Moreover, BMP inhibition promotes Wnt signaling during generation of chondrogenic mesoderm from embryonic stem cells (Tanaka et al., 2009). The HF cells from *Lgr4*cKO mice displayed higher BMP signaling activities at anagen onset than their WT counterparts. Overall, upregulated BMP signaling together with reduced Akt/mTOR and Wnt signaling in *Lgr4*-deficient HFs are consistent with a positive role of LGR4 in promoting LGR5$^+$ HFSC activation during telogen-to-anagen transition.

Our study revealing the important role of LGR4 in the hair cycle and HFSC activation expands the current understanding of the molecular regulation of hair cycle dynamics and stem cell activity. Our work also has important clinical implications for therapeutic advances in hair disorder such as thinning hair and alopecia, as it suggests the LGR4-associated pathway as a potential target for the treatment in the future.

MATERIALS AND METHODS

Animals

Several mice strains (*Lgr4$^{fl/fl}$*, *Lgr5-EGFP* and *Lgr4$^{+/-}$* mice) were gifts from Shanghai Key Laboratory of Regulatory Biology at East China Normal University. *Lgr4$^{+/-}$* mice were generated by gene-trap as described previously (Weng et al., 2008), whereas *K14-Cre* mice (*KRT14-cre*) were purchased from the Jackson Laboratory. Epithelial-specific *Lgr4* knockout mice were obtained by crossing *Lgr4$^{fl/fl}$* mice with *K14-Cre* mice. BALB/c nude mice were purchased from Shanghai SLAC Laboratory Animal Co, Ltd (Shanghai, China). Mice were housed in a specific pathogen-free animal vivarium, and all experiments were approved by the Animal Care and Use Committee at East China Normal University.

β-galactosidase (LacZ) staining

Skin tissues from *Lgr4$^{+/-}$* female mice at different ages were fixed in an ice-cold fixation buffer (2% formaldehyde, 0.2% glutaraldehyde, and 0.02% NP40 in PBS) for 2 hours at 4 °C on a shaking platform. After washing twice in a washing buffer (2 mM MgCl$_2$, 0.01% deoxycholate, and 0.02% NP40 in PBS, pH 8.0), samples were incubated in a staining buffer (0.5 mg/ml X-gal dissolved in LacZ wash buffer) overnight at room temperature. Tissues were then fixed in 4% paraformaldehyde and sectioned for histological analysis.

Patch assay in nude mice

Skin samples from two-month-old *Lgr4*cKO or control female mice were incubated overnight at 4 °C in 0.2% dispase II (Invitrogen, Thermo Fisher Scientific, Waltham, MA) dissolved in DMEM. The epidermis and dermis were separated using forceps and further digested with 0.2% collagenase I (Invitrogen) in PBS for 1 hour at 37 °C. After filtering through a 40-μm strainer, the isolated epidermal cells were collected and counted. A total of 1×10^6 of *Lgr4$^{+/+}$* or *Lgr4$^{-/-}$* epidermal cells were mixed with 1×10^6 fetal dermal cells (1–2 days after birth) and then injected subcutaneously into the dorsal skin of two-month-old nude mice that were anesthetized via intraperitoneal injection of sodium pentobarbital at 1.3 mg/kg body weight. Host mice were killed 3 weeks later and tissues were harvested for analysis.

Skin grafts

After anesthesia with 0.5% sodium pentobarbital at 30 mg/kg body weight, the skin with fur of the *Lgr4*cKO and control female mice (P19) was cut off by an 8-mm diameter puncher. The grafts of the *Lgr4*cKO and control mice were transplanted onto the back of two-month-old BALB/c nude mice. The anastomotic sites were then sutured with 6–7 stitches and dabbed with 0.1% penicillin cotton balls. The stitches were removed 7–10 days

later, and hair growth was analyzed at day 21 after transplantation. Hair number was counted and hair length was measured by a millimeter scale.

Akt activator injection

The *Lgr4*cKO and control female mice at P21 were shaved on the dorsal skin. The WT skin was subcutaneously injected with PBS at 100 μl per day, whereas cKO mice were injected with the same dose of Akt activator SC79 (ApexBio, Houston, TX) at a concentration of 200 μM. Hair growth was monitored by photographing (Canon SX220 HS) every two days.

Statistical analysis

Data were expressed as mean ± SD. Student's *t*-test was used to assess the statistical significance of differences between the groups; *P*-values < 0.05 were considered to be significant.

Supplementary Material

Refer to Web version on PubMed Central for supplementary material.

ACKNOWLEDGMENTS

Data availability statement

No datasets were generated or analyzed during this study.

Abbreviations:

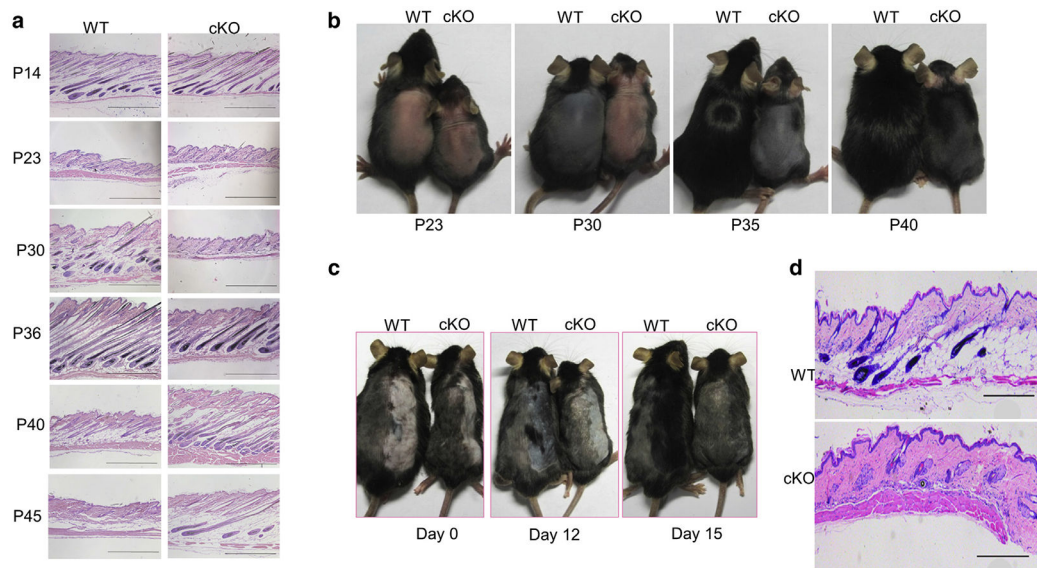|	
Akt	protein kinase B
DP	dermal papilla
HF	hair follicle
HFSC	hair follicle stem cell
HG	hair germ
Lgr4*cKO*	constitutive Lgr4 knockout
P	postnatal day
p-S6	phospho-S6
WT	wild-type

REFERENCES

Bartholomew A, Sturgeon C, Siatskas M, Ferrer K, McIntosh K, Patil S, et al. Mesenchymal stem cells suppress lymphocyte proliferation in vitro and prolong skin graft survival in vivo. Exp Hematol 2002;30:42–8. [PubMed: 11823036]

Carmon KS, Gong X, Lin Q, Thomas A, Liu Q, Liu QJPotNAoS. R-spondins function as ligands of the orphan receptors LGR4 and LGR5 to regulate Wnt/β-catenin signaling. Proc Natl Acad Sci USA 2011;108:11452–7. [PubMed: 21693646]

Deng Z, Lei X, Zhang X, Zhang H, Liu S, Chen Q, et al. mTOR signaling promotes stem cell activation via counterbalancing BMP-mediated suppression during hair regeneration. J Mol Cell Biol 2015;7:62–72. [PubMed: 25609845]

Ehama R, Ishimatsu-Tsuji Y, Iriyama S, Ideta R, Soma T, Yano K, et al. Hair follicle regeneration using grafted rodent and human cells. J Invest Dermatol 2007;127:2106–15. [PubMed: 17429436]

Fuchs E The tortoise and the hair: slow-cycling cells in the stem cell race. Cell 2009;137:811–9. [PubMed: 19490891]

Gong X, Yi J, Carmon KS, Crumbley CA, Xiong W, Thomas A, et al. Aberrant RSPO3-LGR4 signaling in Keap1-deficient lung adenocarcinomas promotes tumor aggressiveness. Oncogene 2015;34:4692–701. [PubMed: 25531322]

Greco V, Chen T, Rendl M, Schober M, Pasolli HA, Stokes N, et al. A two-step mechanism for stem cell activation during hair regeneration. Cell Stem Cell 2009;4:155–69. [PubMed: 19200804]

Kinzel B, Pikiolek M, Orsini V, Sprunger J, Isken A, Zietzling S, et al. Functional roles of Lgr4 and Lgr5 in embryonic gut, kidney and skin development in mice. Dev Biol 2014;390:181–90. [PubMed: 24680895]

Lee SE, Sada A, Zhang M, McDermitt DJ, Lu SY, Kemphues KJ, et al. High Runx1 levels promote a reversible, more-differentiated cell state in hair-follicle stem cells during quiescence. Cell Rep 2014;6:499–513. [PubMed: 24462289]

Li N, Liu S, Zhang HS, Deng ZL, Zhao HS, Zhao Q, et al. Exogenous R-Spondin1 induces precocious telogen-to-anagen transition in mouse hair follicles. Int J Mol Sci 2016;17:582.

Liang F, Yue J, Wang J, Zhang L, Fan R, Zhang H, et al. GPCR48/LGR4 promotes tumorigenesis of prostate cancer via PI3K/Akt signaling pathway. Med Oncol 2015;32:49. [PubMed: 25636507]

Lien WH, Fuchs E. Wnt some lose some: transcriptional governance of stem cells by Wnt/β-catenin signaling. Genes Dev 2014;28:1517–32. [PubMed: 25030692]

Lim X, Tan SH, Yu KL, Lim SBH, Nusse R. Axin2 marks quiescent hair follicle bulge stem cells that are maintained by autocrine Wnt/β-catenin signaling. Proc Natl Acad Sci USA 2016;113:E1498–505. [PubMed: 26903625]

Lin CL, Xu R, Yi JK, Li F, Chen J, Jones EC, et al. Alkaline ceramidase 1 protects mice from premature hair loss by maintaining the homeostasis of hair follicle stem cells. Stem Cell Rep 2017;9:1488–500.

Lin HY, Yang LT. Differential response of epithelial stem cell populations in hair follicles to TGF-β signaling. Dev Biol 2013;373:394–406. [PubMed: 23103542]

Lowry WE, Blanpain C, Nowak JA, Guasch G, Lewis L, Fuchs E. Defining the impact of beta-catenin/Tcf transactivation on epithelial stem cells. Genes Dev 2005;19:1596–611. [PubMed: 15961525]

Luo J, Zhou W, Zhou X, Li D, Weng J, Yi Z, et al. Regulation of bone formation and remodeling by G-protein-coupled receptor 48. Development 2009;136:2747–56. [PubMed: 19605502]

Matsumura H, Mohri Y, Binh NT, Morinaga H, Fukuda M, Ito M, et al. Hair follicle aging is driven by transepidermal elimination of stem cells via COL17A1 proteolysis. Science 2016;351:aad4395. [PubMed: 26912707]

Mohri Y, Kato S, Umezawa A, Okuyama R, Nishimori K. Impaired hair placode formation with reduced expression of hair follicle-related genes in mice lacking Lgr4. Dev Dyn 2008;237:2235–42. [PubMed: 18651655]

Oshimori N, Fuchs E. Paracrine TGF-β signaling counterbalances BMP-mediated repression in hair follicle stem cell activation. Cell Stem Cell 2012;10:63–75. [PubMed: 22226356]

Qiu W, Lei M, Zhou L, Bai X, Lai X, Yu Y, et al. Hair follicle stem cell proliferation, Akt and Wnt signaling activation in TPA-induced hair regeneration. Histochem Cell Biol 2017;147:749–58. [PubMed: 28185006]

Schneider MR, Schmidt-Ullrich R, Paus R. The hair follicle as a dynamic miniorgan. Curr Biol 2009;19:R132–42. [PubMed: 19211055]

Siwko S, Lai L, Weng J, Liu M. Lgr4 in ocular development and glaucoma. J Ophthalmol 2013;2013:987494. [PubMed: 23840940]

Smith AA, Li J, Liu B, Hunter D, Pyles M, Gillette M, et al. Activating hair follicle stem cells via R-spondin2 to stimulate hair growth. J Invest Dermatol 2016;136:1549–58. [PubMed: 27109869]

Tanaka M, Jokubaitis V, Wood C, Wang Y, Brouard N, Pera M, et al. BMP inhibition stimulates WNT-dependent generation of chondrogenic mesoderm from embryonic stem cells. Stem Cell Res 2009;3:126–41. [PubMed: 19700382]

Trempus CS, Morris RJ, Ehinger M, Elmore A, Bortner CD, Ito M, et al. CD34 expression by hair follicle stem cells is required for skin tumor development in mice. Cancer Res 2007;67:4173–81. [PubMed: 17483328]

Wang X, Chen H, Tian R, Zhang Y, Drutskaya MS, Wang C, et al. Macrophages induce AKT/β-catenin-dependent Lgr5+ stem cell activation and hair follicle regeneration through TNF. Nat Commun 2017;8:14091. [PubMed: 28345588]

Weng J, Luo J, Cheng X, Jin C, Zhou X, Qu J, et al. Deletion of G protein-coupled receptor 48 leads to ocular anterior segment dysgenesis (ASD) through down-regulation of Pitx2. Proc Natl Acad Sci USA 2008;105:6081–6. [PubMed: 18424556]

Xu P, Dang Y, Wang L, Liu X, Ren X, Gu J, et al. Lgr4 is crucial for skin carcinogenesis by regulating MEK/ERK and Wnt/β-catenin signaling pathways. Cancer Lett 2016;383:161–70. [PubMed: 27693558]

Yue Z, Yuan Z, Zeng L, Wang Y, Lai L, Li J, et al. LGR4 modulates breast cancer initiation, metastasis, and cancer stem cells. FASEB J 2018;32:2422–37. [PubMed: 29269400]

Zhang J, He XC, Tong WG, Johnson T, Wiedemann LM, Mishina Y, et al. Bone morphogenetic protein signaling inhibits hair follicle anagen induction by restricting epithelial stem/progenitor cell activation and expansion. Stem Cells 2006;24:2826–39. [PubMed: 16960130]

Figure 1. LGR4 expression in postnatal HFs.

(**a**) β-galactosidase staining of skin in *Lgr4*^{+/−} mice at P17, P19, P23, P25, P27, P36, P55, and P65. Bar = 100 μm. (**b**) Quantitative analysis for LacZ staining in (a). Data were expressed as IOD of LacZ staining. n = 3. (**c**) RT-PCR analysis revealing dynamic changes of *Lgr4* mRNA expression in WT mouse skin, normalized to *GAPDH*. Data are expressed as mean ± SD from three independent experiments. Bu, bulge; DP, dermal papilla; HF, hair follicle; HG, secondary hair germ; IE, interfollicular epidermis; IOD, integrated optical density; IRS, inner root sheath; Mx, matrix; ns, not significant; ORS, out root sheath; P, postnatal day; SG, sebaceous gland; WT, wild-type. *$P < 0.05$, **$P < 0.01$.

Figure 2. *Lgr4* deficiency delays hair cycle.
(**a**) Representative images of H&E staining of skin in *Lgr4*cKO and control mice at the indicated ages. Bar = 200 μm. (**b**) Representative images showing skin color and hair regrowth in control (left) and *Lgr4*cKO (right) mice at P23, P30, P35, and P40, following shaving of dorsal skin. (**c**) *Lgr4* deletion slows down depilation-induced hair regrowth in 18-month-old mice. Images at the indicated time point after shaving (left of the dorsal skin, as a control) and depilation (right of the dorsal skin) are shown. (**d**) Representative images of H&E staining of skin in *Lgr4*cKO and WT mice at day 12 after depilation. Bar = 400 μm. cKO, constitutive knockout; P, postnatal day; WT, wild-type.

Figure 3. *Lgr4* deficiency inhibits HSFC activation.
(**a**) FACS analysis (left) and quantification (right) of LGR5^{+} HFSCs from *Lgr4*^{+/+} and *Lgr4*^{−/−} mouse epidermis with LGR5 GFP reporter at P25. (**b**) Representative immunofluorescence images and quantitative analysis of GFP-positive cells per HF in P25 skin of *Lgr4*cKO and control mice. Bar = 100 μm (left). Bar = 20 μm (right). (**c**) Immunofluorescence images for P-cadherin staining in HFs of *Lgr4*cKO and control mice at P23, P25, and P27. Bar = 100 μm. (**d**) Representative images of Ki67 immunostaining (upper) and quantification of Ki67^{+} cells (lower) in P25 skin of *Lgr4*cKO and control mice. Data are expressed as mean ± SD of three independent experiments. *$P < 0.05$, ***$P < 0.001$, control versus cKO. Bar = 100 μm (left). Bar = 20 μm (right). cKO, constitutive knockout; HF, hair follicle; HFSC, hair follicle stem cell; P, postnatal day; WT, wild-type.

Figure 4. *Lgr4* deletion inhibits hair and HF regeneration upon transplantation.
(**a**) Experimental design and (**b**) representative images of HF reconstitution by subcutaneous epidermal and dermal cell injection. (**c**) Quantitative analysis of hair number in the grafts from *Lgr4*cKO and control epidermal cells. n = 6, *P < 0.05, control versus cKO.
(**d**) Representative images showing hair growth at day 21 after transplanting hairs from *Lgr4*cKO and control mice to the back of nude mice. (**e**) Hair number per pinch in skin transplants from *Lgr4*cKO and control mice was quantified. (**f**) Average hair length in skin transplants from *Lgr4*cKO and control mice was measured using a millimeter scale. n = 3, *P < 0.01, control versus cKO. cKO, conditional knockout; HF, hair follicle; ns, not significant; WT, wild-type.

Figure 5. *Lgr4* deletion alters the activity of Akt, Wnt, and BMP signaling in HF.
(**a**) Immunostaining for p-S6 in skin at P23, P25, and P27. Bar = 100 μm. (**b**) Western blot analysis of p-S6, β-SMAD1/5/9, and β-catenin in skin at P25. (**c**) Target gene expressions of Akt signaling in CD34⁺α6-integrin⁺ HFSCs at P23. Data are expressed as mean ± SD. n = 3, *P < 0.05, **P < 0.01, control versus cKO. (**d**) The WT skin at P21 was subcutaneously injected with PBS at 100 μl, whereas the cKO skin was injected with 200 μM Akt activator SC79. (**e**) Immunostaining for β-catenin in skin at P23, P25, and P27. Bar = 100 μm. (**f**) Images of immunofluorescence staining for LEF1 in *Lgr4*cKO and control mice at P30. Bar = 100 μm. (**g**) Target gene expressions of Wnt signaling in CD34⁺α6-integrin⁺ HFSCs at P23. Data are expressed as mean ± SD. n = 3, *P < 0.05, **P < 0.01, control versus cKO. Akt, protein kinase B; cKO, constitutive knockout; HF, hair follicle; HFSC, hair follicle stem cell; P, postnatal day; p-S6, phospho-S6; WT, wild-type.